

## Morphology development of elongated $\alpha$ phases in hot working of large-scale titanium alloy plate

Xiao-guang FAN, He YANG, Peng-fei GAO, Si-liang YAN

State Key Laboratory of Solidification Processing, School of Materials Science and Engineering,  
Northwestern Polytechnical University, Xi'an 710072, China

Received 19 December 2012; accepted 13 March 2013

**Abstract:** The role of subtransus hot working on microstructure morphology of TA15 titanium alloy plate with elongated  $\alpha$  phases was studied by quantitative metallography on different sections. The results show that the microstructure morphology is mainly affected by loading direction. When the sample is compressed along normal direction, microstructure on the section vertical to normal direction has equiaxed primary  $\alpha$  phase but microstructure on the section vertical to rolling direction has strip primary  $\alpha$  phase with long axis along tangential direction. When the sample is compressed along rolling direction, microstructure on the section vertical to normal direction has strip primary  $\alpha$  phase elongated along tangential direction but microstructure on the section vertical to rolling direction consists of strip and irregular broad-band primary  $\alpha$  phase. The strip primary  $\alpha$  phase aspect ratio is smaller at lower temperature due to the dynamic break-down of  $\alpha$  phase. The difference on primary  $\alpha$  phase aspect ratio between different sections decreases after compression along distinct directions in two loading passes, suggesting the improvement of equiaxity of primary  $\alpha$  phase.

**Key words:** microstructure morphology; TA15 titanium alloy; elongated  $\alpha$  phases; subtransus hot working

### 1 Introduction

Titanium alloys have high specific strength, superior creep resistance, good thermal stability and excellent corrosion resistance, so they are widely used to manufacture structural components in aviation and aerospace industries. To satisfy the increasing demands of light mass and high performance, large scale components with complex shape are often required. Meanwhile, these components often serve as key load-bearing structure in severe conditions, therefore, specific microstructure is needed to obtain the required service performance [1–8]. Thus, one important aim of hot working is to tailor the microstructure of the large scale complex titanium components through process design.

Typically, the thermo-mechanical processing of titanium alloys components involves primary processing in which ingots are converted into semi-products (e.g., plates and rods), and secondary processing for shaping

semi-products into finished components [9,10]. Commonly, the initially equiaxed microstructure is necessary to obtain desired microstructure in the final forging. However, the microstructure with pancaked or elongated primary  $\alpha$  phase is often produced due to improper processing in the primary hot working, especially when the semi-product is large. The elongated  $\alpha$  phases may result in strong anisotropy and degraded fatigue performance. In addition, it is well known that the microstructure of titanium alloys is very sensitive to processing [9,11,12]. It is possible to transform the elongated  $\alpha$  phases into finely equiaxed microstructure by proper thermo-mechanical processing, such that the service performance of the final products can be enhanced.

By now, extensive investigations have been carried out on the microstructure evolution and relationship between processing parameters and microstructure in the subtransus hot working of titanium alloys. However, most studies are focused on the microstructure evolution of titanium alloys with initially equiaxed microstructure

during the final forging [13–17]. The objective of the present work is to study the microstructure morphology of titanium alloys with elongated  $\alpha$  phases under different processing conditions in the subtransus hot working so as to provide basis for the transformation from elongated  $\alpha$  phases into equiaxed microstructure. To this end, a series of hot compression experiments are conducted in  $\alpha+\beta$  region under different processing parameters (deformation temperature, deformation amount, and loading direction) on the TA15 titanium alloy with elongated  $\alpha$  phases. The microstructure morphology and parameters are observed and quantitatively analyzed on different sections.

## 2 Experimental

The material used in this investigation is a near  $\alpha$  TA15 titanium alloy (Ti–6Al–2Zr–1Mo–1V) with the measured  $\beta$ -transus temperature 990 °C. The TA15 alloy was supplied in hot rolled plate with specification of 1200 mm  $\times$  280 mm  $\times$  80 mm. The initial microstructure is shown in Fig. 1. It can be seen that the microstructure on section vertical to normal direction (ND) consists of equiaxed primary  $\alpha$  phase and transformed  $\beta$  matrix. The microstructure on section vertical to rolling direction (RD) and section vertical to tangential direction (TD) have close morphology. They are both composed of elongated primary  $\alpha$  phase and transformed  $\beta$  matrix. The measured content and aspect ratio of primary  $\alpha$  phase ( $\alpha_p$ ) are listed in Table 1. From the microstructure morphology on different sections, it can be concluded that the initial microstructures have pancake-shaped  $\alpha$  grains with its normal direction parallel to the normal direction of initial plate.

Two kinds of cuboid specimens with the same dimension (25 mm  $\times$  17 mm  $\times$  15 mm) but different orientations were machined from the rolled TA15 plate, as shown in Fig. 2. Specimen A was cut with the longest side parallel to the normal direction and the shortest side parallel to the rolling direction. While specimen B was cut with the longest side parallel to the rolling direction and the shortest side parallel to the normal direction. In the isothermal compression tests, the sample was heated to deformation temperature at heating rate of 12 °C/min and held for 30 min. After that, the sample was compressed along the prescribed direction at the constant nominal strain rate of 0.01 s<sup>-1</sup> to a certain deformation degree and then air-cooled. As the initial microstructure have pancake-shaped  $\alpha$  grains, the deformed microstructure morphology may vary with loading direction. Thus, different loading schemes were proposed in this work. Considering the close microstructure morphology on RD-section and TD-section, the compression along tangential direction and the

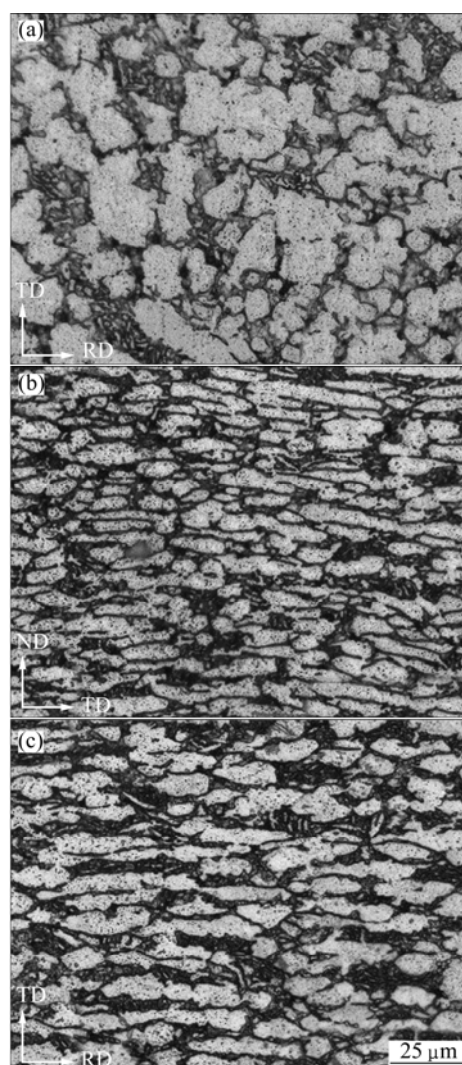


**Fig. 1** Microstructures of as-received TA15 titanium alloy plate: (a) ND-section; (b) RD-section; (c) TD-section

**Table 1** Quantitatively measured microstructure parameters of initial microstructure of TA15 alloy

Section	Content of $\alpha_p$ /%	Aspect ratio of $\alpha_p$
ND	61.53	1.85
RD	57.63	3.29
TD	55.59	3.20

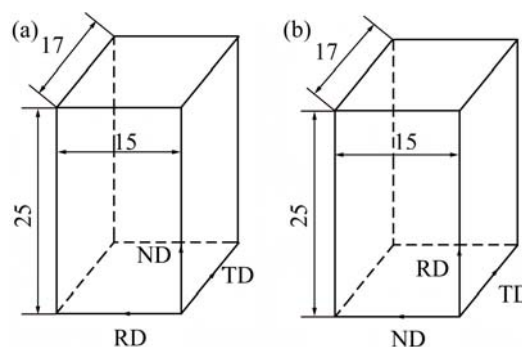


**Fig. 2** Schematic of specimen: (a) Specimen A; (b) Specimen B

microstructure sectioned vertical to tangential direction are not considered in this work. The detailed processing parameters are listed in Table 2. For tests 9 and 10, the sample was compressed to the degree of 55% along the prescribed loading direction in sequence in two loading pass. The bulging of deformed sample produced in the first loading pass was removed before the second loading pass.

**Table 2** Isothermal compression experiment scheme

No.	Specimen type	Deformation temperature/°C	Loading direction	Deformation degree/%
1	A	960	ND	80
2	A	920	ND	80
3	A	880	ND	80
4	B	960	RD	80
5	B	920	RD	80
6	B	880	RD	80
7	A	920	ND	55
8	B	920	RD	55
9	A	920	ND→RD	55
10	B	920	RD→ND	55

The microstructure of forged sample was observed on the ND-section and RD-section using Leica DMI 3000 optical microscope. Metallographic preparation of the specimens was carried out by mechanically grinding with SiC paper and polishing with a solution of water and Cr<sub>2</sub>O<sub>3</sub> polisher, and etching with a solution of 13% HNO<sub>3</sub>+7% HF+80% H<sub>2</sub>O. The content, grain size and aspect of primary  $\alpha$  phase were quantitatively measured using Image-pro Plus software. The content of primary  $\alpha$  phase is the ratio of all  $\alpha$  grains area to total area of image. For one  $\alpha$  grain, the grain size is the average length of diameters measured at 2° intervals and passing through grain's centroid, and the aspect is the ratio between major axis and minor axis of ellipse equivalent to grain. The grain size and aspect of primary  $\alpha$  phase mentioned below is the average value of all  $\alpha$  grains.

### 3 Results and discussion

#### 3.1 Microstructure at different deformation temperatures and loading directions

The microstructure of samples compressed along ND to the deformation degree of 80% at different temperatures is shown in Fig. 3. The corresponding microstructural parameters are listed in Table 3. As shown in Fig. 3, the microstructure mainly consists of primary  $\alpha$  phase and transformed  $\beta$  matrix, which is the same as that of the initial microstructure. It can be seen from Table 3 that the content of primary  $\alpha$  phase on different sections are close at a certain deformation temperature. It is found that the primary  $\alpha$  phase content

decreases with the increase of temperature, and the content of primary  $\alpha$  phase at 920 °C is not far from that at 880 °C but is much greater than that at 960 °C. This is related to the law of  $\alpha \rightarrow \beta$  phase transformation of TA15 titanium alloy in  $\alpha + \beta$  region, i.e. the primary  $\alpha$  phase content decreases slowly with increasing temperature in the lower  $\alpha + \beta$  region, but decreases rapidly with temperature in the upper  $\alpha + \beta$  region [18,19].

When the sample is compressed along ND, the initial pancake-shaped  $\alpha$  grains are flattened further and keep the pancake shape. So the microstructures of samples compressed along ND at different temperatures all have the same morphology as the initial microstructure with near equiaxed primary  $\alpha$  phase on the ND-section and strip primary  $\alpha$  phase with long axis along tangential direction on the RD-section (Figs. 1 and 3). However, the microstructure parameters vary with the deformation temperature. Using the average diameter of primary  $\alpha$  grain on the ND-section to represent the size of pancake-shaped primary  $\alpha$  grain, the grain size of primary  $\alpha$  at different temperatures are listed in Table 3. It can be seen that the primary  $\alpha$  grain size at 920 °C is greater than that of the initial microstructure (7.15  $\mu\text{m}$ ), but those at 960 and 880 °C are smaller compared to the initial microstructure. This may be caused by the couple effect of flattening of primary  $\alpha$  grain,  $\alpha \rightarrow \beta$  phase transformation and the dynamic break-down of  $\alpha$  phase. The initial pancake-shaped  $\alpha$  grain would be flattened during the deformation along ND, resulting in the increase of primary  $\alpha$  grain size. However, as mentioned above, the primary  $\alpha$  phase content decreases rapidly with temperature increasing in the upper  $\alpha + \beta$  region, which would diminish the grain size of primary  $\alpha$  markedly. In addition, the primary  $\alpha$  particles act as hard inclusions in the soft  $\beta$  matrix and are harder to deform than  $\beta$  phase in the subtransus hot working [20,21]. Considering the  $\alpha \rightarrow \beta$  phase transformation with increasing temperature, it can be concluded that the higher the deformation temperature is, the less the primary  $\alpha$  phase takes part in deformation and bears smaller deformation. So at higher temperature (960 °C), the primary  $\alpha$  grain size is mainly determined by the  $\alpha \rightarrow \beta$  phase transformation, leading to the smaller grain size than that of the initial microstructure. With the temperature decreasing, the effect of  $\alpha \rightarrow \beta$  phase transformation on grain size decreases and the flattening of primary  $\alpha$  phase plays a more important role in the grain size change of primary  $\alpha$  phase. Thus, the grain size of primary  $\alpha$  of sample deformed at 920 °C is greater than that of the initial microstructure. The primary  $\alpha$  aspect ratio on RD-section of sample deformed at 920 °C is greater than that of the initial microstructure, which confirms the speculation above. The dynamic break-down of  $\alpha$  phase is also an important

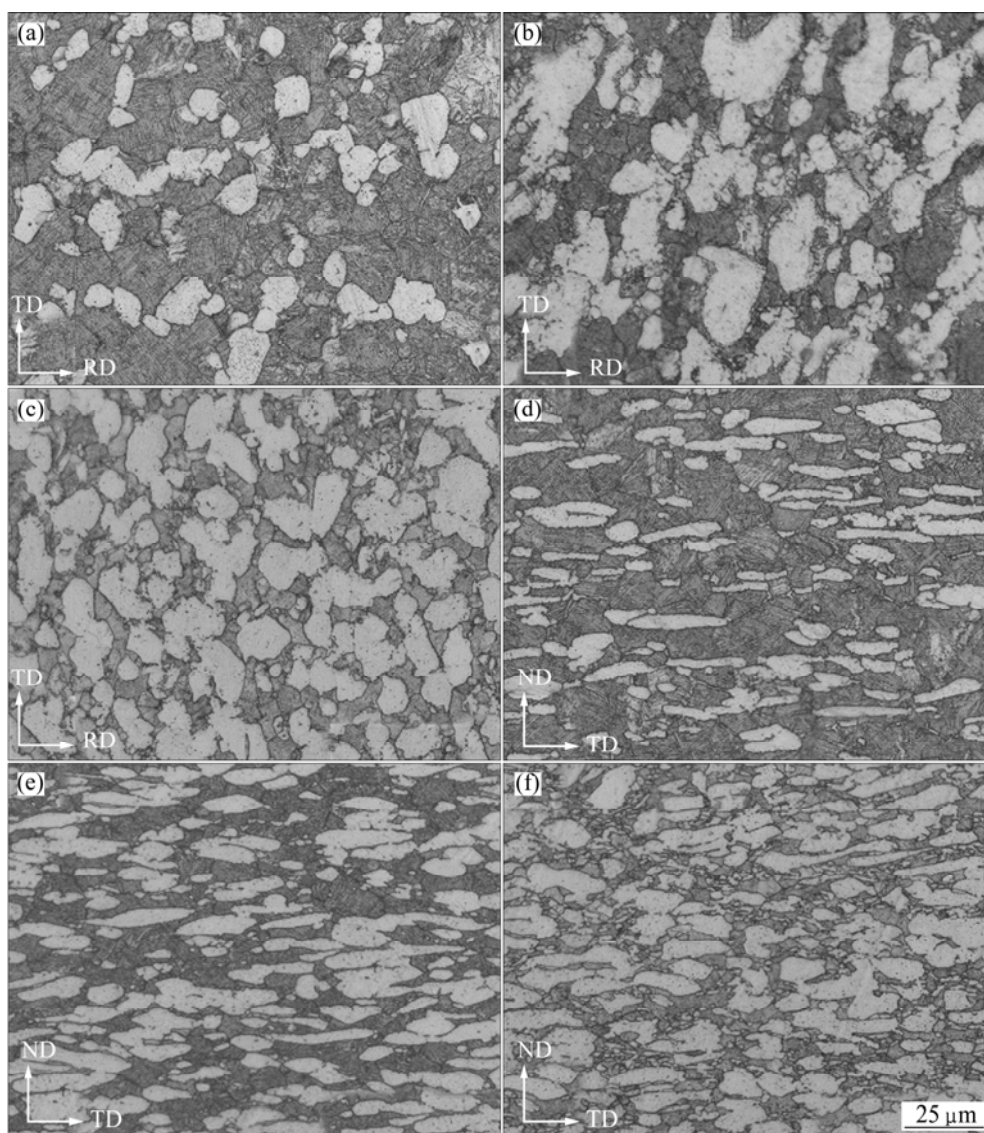


**Fig. 3** Microstructures of samples compressed along ND to deformation degree of 80% at different temperatures: (a) 960 °C, ND-section; (b) 920 °C, ND-section; (c) 880 °C, ND-section; (d) 960 °C, RD-section; (e) 920 °C, RD-section; (f) 880 °C, RD-section

**Table 3** Quantitatively measured microstructure parameters of samples compressed along different directions to deformation degree of 80% at different temperatures

Compression direction	Temperature/°C	ND-section			RD-section	
		Content of $\alpha_p$ /%	Aspect ratio of $\alpha_p$	Grain size of $\alpha_p/\mu\text{m}$	Content of $\alpha_p$ /%	Aspect ratio of $\alpha_p$
ND	960	28.62	1.90	6.16	27.74	3.75
	920	46.99	1.73	7.76	45.67	3.81
	880	55.77	1.91	6.57	53.08	2.81
RD	960	32.63	2.86	–	30.53	2.57
	920	50.03	3.09	–	47.21	2.49
	880	52.26	2.39	–	54.09	2.54

mechanism during hot working of titanium alloy. When the temperature decreases to 880 °C, the primary  $\alpha$  phase would undergo larger deformation due to less soft  $\beta$  phase, so that the break-down of  $\alpha$  phase plays more

significant role in the grain size change of primary  $\alpha$  phase than that of the compression of  $\alpha$  phase. As a result, the grain size of primary  $\alpha$  of sample deformed at 880 °C is smaller than those of the initial microstructure and the

sample deformed at 920 °C. The dynamic break-down would also decrease the aspect ratio of primary  $\alpha$  phase, so the primary  $\alpha$  aspect ratio on RD-section of sample deformed at 880 °C is smaller than those of the initial microstructure and the sample deformed at 920 °C.

Figure 4 shows the microstructure of samples compressed along RD to the deformation degree of 80% at different temperatures, of which the corresponding microstructural parameters are listed in Table 3. Similar to the microstructure of samples compressed along ND, the microstructure is mainly composed of primary  $\alpha$  phase and transformed  $\beta$  matrix. From Table 3, it can be seen that the content of primary  $\alpha$  phase varies little with the section at a certain temperature and is close to that of sample compressed along ND at the same temperature, suggesting that the loading direction has little effect on

the content of primary  $\alpha$  phase.

It can be found from Fig. 4 that the microstructure presents different morphology compared with that deformed along ND (Fig. 3). On one hand, the microstructure on ND-section has strip primary  $\alpha$  phase elongated along tangential direction. On the other hand, the microstructure on RD-section is non-uniform, which consists of strip primary  $\alpha$  phase and irregular broad-band primary  $\alpha$  phase. This can be explained by the morphology evolution of primary  $\alpha$  phase during deformation. When the sample is compressed along RD, the initial pancake-shaped  $\alpha$  grains are compressed on the side along the long axis. Under large deformation, the primary  $\alpha$  grains may be upset and further flattened at the rolling direction and get bulge at the normal direction. So the primary  $\alpha$  grains on ND-section are strip-shape with

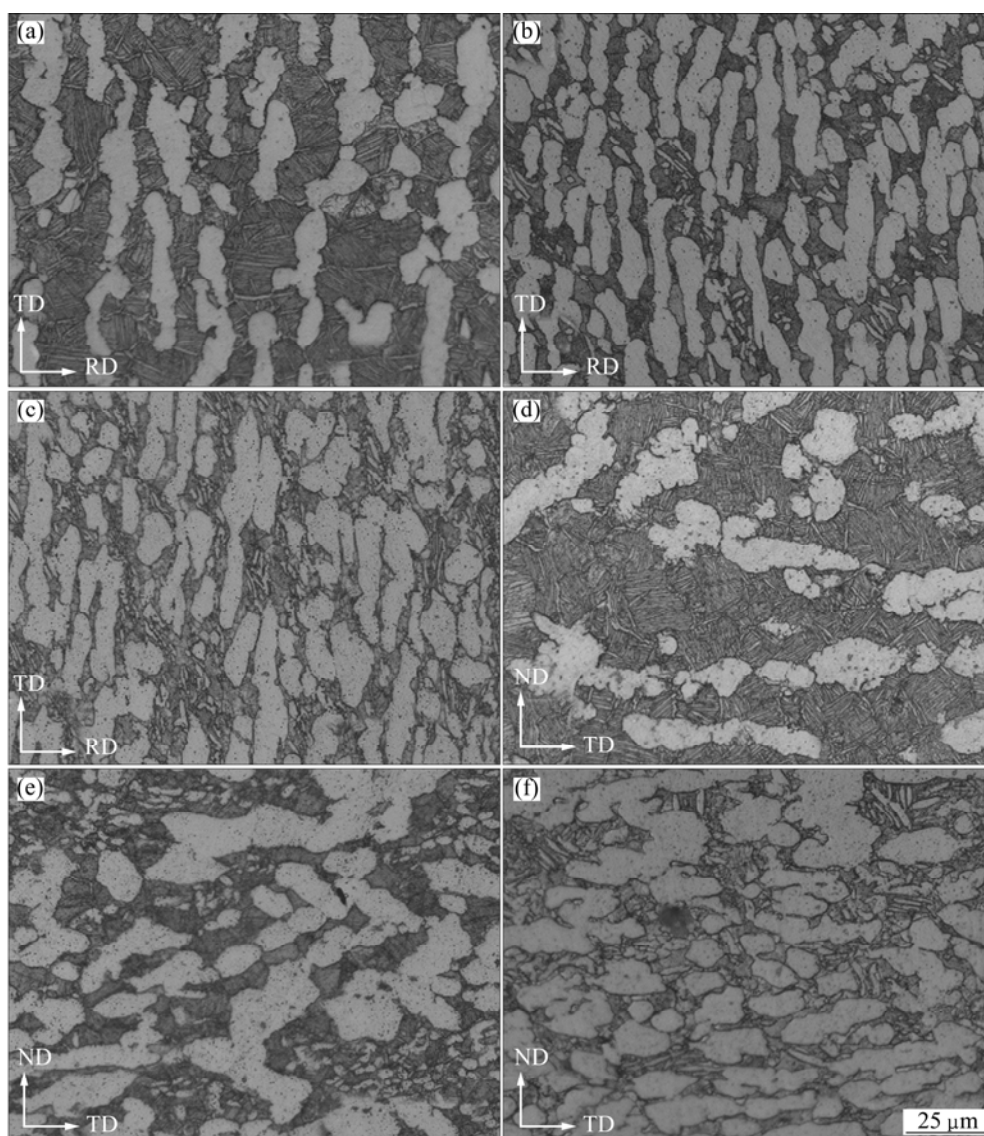


**Fig. 4** Microstructures on different sections of samples compressed along RD to deformation degree of 80% at different temperatures: (a) 960 °C, ND-section; (b) 920 °C, ND-section; (c) 880 °C, ND-section; (d) 960 °C, RD-section; (e) 920 °C, RD-section; (f) 880 °C, RD-section

long axis along tangential direction, and the primary  $\alpha$  grains on RD-section are thicker than that in the initial microstructure (Fig. 1(b)). In addition, some thinner initial pancake-shaped  $\alpha$  grains may be bent and kinked resulting in complex 3D morphology during deformation. So some irregular broad-band primary  $\alpha$  grains exist in the microstructure on RD-section leading to nonuniform morphology. However, this phenomenon has little effect on the morphology of primary  $\alpha$  grains on ND-section. As mentioned above, the primary  $\alpha$  particles are harder to deform than  $\beta$  phase and bear larger deformation at low temperature. As a result, the aspect ratio of primary  $\alpha$  on ND-section of sample deformed at 920 °C is greater than that of sample deformed at 960 °C (Table 3). But the primary  $\alpha$  aspect ratio on ND-section of sample deformed at 880 °C is less than those of samples deformed at 960 and 920 °C, which does not follow the regularity above. This is caused by the significant dynamic break-down of  $\alpha$  phase at 880 °C. Dynamic recrystallization plays an important role in the break-down of  $\alpha$  phase, especially when the deformation takes

place in the lower two phase region. HE et al [22] investigated the deformation mechanism of TA15 alloy with initially equiaxed structure. They reported significant dynamic recrystallization for the TA15 alloy at temperature of 850 °C and strain rates of 0.1–0.001 s<sup>-1</sup>. In the present work, the deformation temperature and strain rate are similar to those in Ref. [22]. However, the strain is much higher, which promotes dynamic recrystallization. Thus, the aspect ratio of  $\alpha$  phase decreases.

### 3.2 Microstructure at different deformation degrees and loading directions

The microstructures of samples compressed along different directions to the deformation degree of 55% at 920 °C are shown in Fig.5. The corresponding microstructural parameters are listed in Table 4. By comparing the microstructure with different deformation degrees (Figs. 3(b,e), Figs. 4(b,e) and Fig. 5), the effect of deformation degree on the microstructure is analyzed in this section.

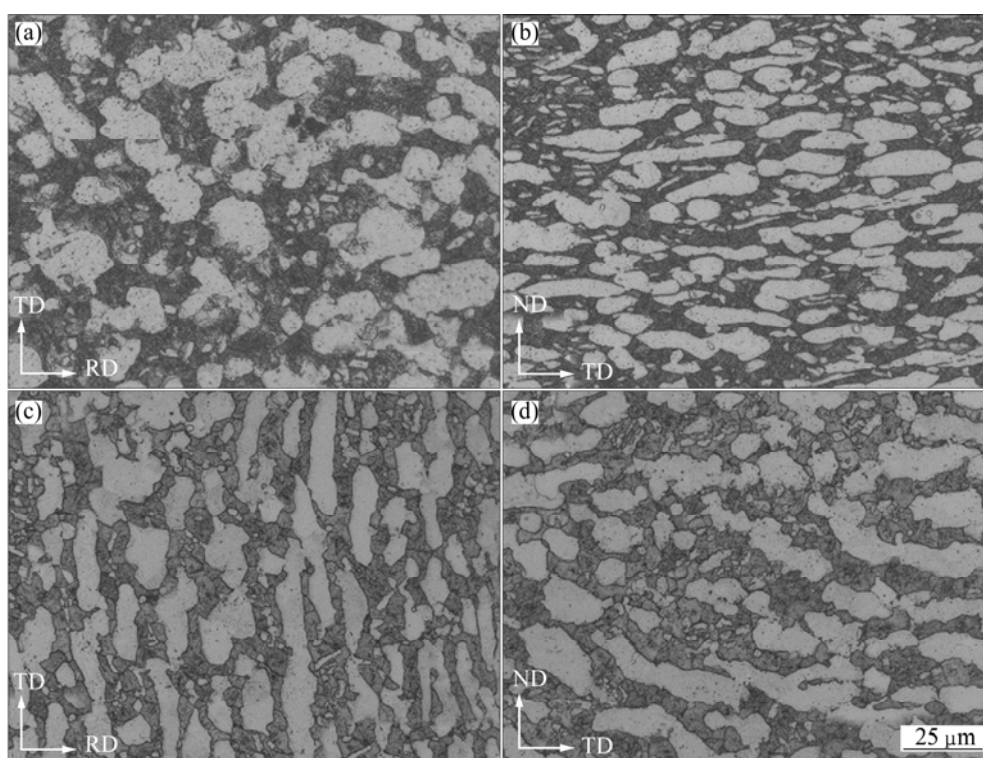


**Fig. 5** Microstructures on different sections of samples compressed along different directions to deformation degree of 55% at 920 °C: (a) ND loading, ND-section; (b) ND loading, RD-section; (c) RD loading, ND-section; (d) RD loading, RD-section

**Table 4** Quantitatively measured microstructure parameters of samples compressed along different directions to deformation degree of 55% at 920 °C

Compression direction	ND-section			RD-section	
	Content of $\alpha_p$ /%	Aspect ratio of $\alpha_p$	Grain size of $\alpha_p$ /μm	Content of $\alpha_p$ /%	Aspect ratio of $\alpha_p$
ND	50.23	1.97	7.41	48.78	3.47
RD	48.71	2.59	–	48.91	2.51

In the case of microstructure constituent and morphology, for each loading direction, no distinction exists between the samples with different deformation degrees. This suggests that the microstructure morphology is mainly determined by loading direction but little affected by deformation degree under the condition of this work.

From Tables 3 and 4, it can be found that the grain size on ND-section with smaller deformation degree is less than that with larger deformation degree for the sample compressed along ND. It was mentioned in Section 3.1 that the pancake-shaped primary  $\alpha$  grain would be flattened and upsetted during the compression along ND. As the deformation degree increases, the primary  $\alpha$  grains would be flattened and upsetted to a larger extent, leading to more significant increase of the cross-section perpendicular to the compression direction (ND direction). So the sample compressed to a smaller degree along ND has smaller grain size on ND-section. For the same reason, the sample compressed to smaller deformation degree along ND has smaller primary  $\alpha$  aspect ratio on RD-section compared to that with larger deformation (Tables 3 and 4). For the sample compressed along RD, the microstructure on ND-section has greater primary  $\alpha$  aspect ratio at larger deformation.

### 3.3 Microstructure at deformation in two directions in sequence

Figure 6 shows the microstructures of samples compressed along different loading directions to the deformation degree of 55% in sequence in two loading passes at 920 °C whose microstructural parameters are listed in Table 5. For Sample 9 compressed along ND and RD in sequence, the microstructure close to the initial microstructure is produced in the first compression along ND, as shown in Figs. 5(a, b). Thus, the second compression of Sample 9 is analogous to the compression of Sample 8 with similar initial microstructure. As a result, Sample 9 compressed along ND and RD in sequence presents the similar microstructure as Sample 8 (Figs. 5(c, d) and Figs. 6(a, b)). In addition, the microstructural parameters of Samples 9 and 8 are also close, as listed in Tables 4 and 5.

For Sample 10 compressed along RD and ND in sequence, the microstructure after first compression along RD is shown in Figs. 5(c, d). In the second compression along ND, the complex primary  $\alpha$  grains generated in the first compression would undergo sophisticated morphology evolution and some  $\alpha$  grains may be broken down during deformation. From Tables 4 and 5, it can be found that primary  $\alpha$  aspect ratio on

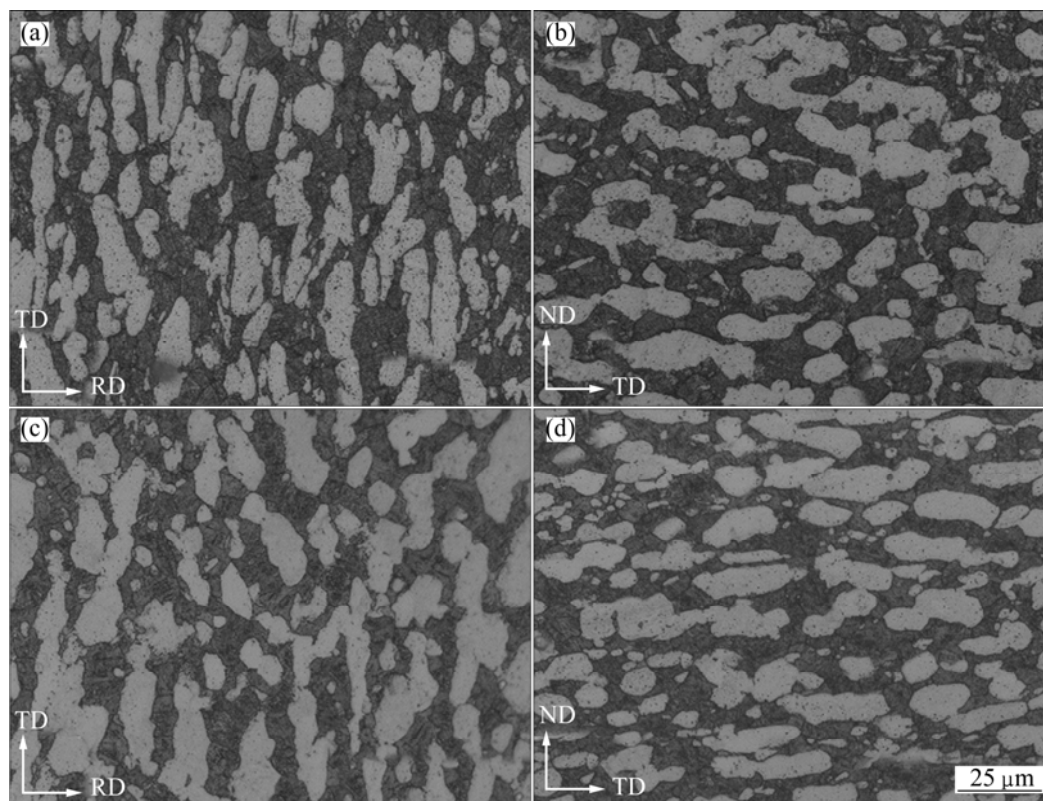


**Fig. 6** Microstructures of samples compressed along different loading directions to deformation degree of 55% in sequence in two loading passes at 920 °C: (a) ND loading→RD loading, ND-section; (b) ND loading→RD loading, RD-section; (c) RD loading→ND loading, ND-section; (d) RD loading→ND loading, RD-section

**Table 5** Quantitatively measured microstructure parameters of samples compressed along different directions to deformation degree of 55% in sequence in two loading passes at 920 °C

Loading direction	ND-section		RD-section	
	Content of $\alpha_p$ /%	Aspect ratio of $\alpha_p$	Content of $\alpha_p$ /%	Aspect ratio of $\alpha_p$
	$\alpha_p$ /%	of $\alpha_p$	$\alpha_p$ /%	of $\alpha_p$
ND→RD	45.69	2.53	46.58	2.42
RD→ND	49.16	2.37	48.81	2.80

ND-section and RD-section after the second compression are both a little smaller than those after the first compression. This may be related to the break-down of primary  $\alpha$  grains. By comparing Fig. 5(d) and Fig. 6(d), it can be seen that lots of strip primary  $\alpha$  phase elongated along tangential direction occurs again after second compression.

Comparing Fig. 1 and Figs. 6(c, d), the change of microstructure can be seen after compression along RD and ND in sequence compared with the initial microstructure. The equiaxed primary  $\alpha$  phase on ND-section in initial microstructure transforms to strip primary  $\alpha$  phase after deformation. The strip primary  $\alpha$  phase on RD-section in initial microstructure still maintains the strip-shape but the aspect ratio of strip primary  $\alpha$  phase decreases after deformation. Besides, the difference on primary  $\alpha$  phase aspect ratio between ND-section and RD-section drops after deformation (Tables 1 and 5), suggesting that the equiaxity of primary  $\alpha$  phase is improved after deformation.

From the above results and analysis, it can be concluded that the microstructure morphology are significantly affected by the loading direction but little affected by the deformation temperature and degree. The microstructures of samples compressed along ND present near equiaxed primary  $\alpha$  phase on the ND-section and strip primary  $\alpha$  phase with long axis along tangential direction on the RD-section. The microstructure of samples compressed along RD presents strip primary  $\alpha$  phase elongated along tangential direction on ND-section and nonuniform microstructure consists of strip primary  $\alpha$  phase and irregular broad-band primary  $\alpha$  phase on RD-section. In addition, the equiaxity of primary  $\alpha$  phase is improved after compression along different directions in two loading passes. So, it can be speculated that the elongated  $\alpha$  phases of TA15 titanium alloy can be transformed to equiaxed microstructure through multi-directional forging.

## 4 Conclusions

1) The microstructure morphology is mainly determined by the loading direction but little affected by the deformation temperature and degree within the

temperature range of 880–960 °C. When the sample is compressed along normal direction, the microstructure on ND-section has near equiaxed primary  $\alpha$  phase but the microstructure on RD-section has strip primary  $\alpha$  phase with long axis along tangential direction. When the sample is compressed along rolling direction, the microstructure on ND-section has strip primary  $\alpha$  phase elongated along tangential direction but the microstructure on RD-section consists of strip primary  $\alpha$  phase and irregular broad-band primary  $\alpha$  phase.

2) At lower temperature (880 °C), the strip primary  $\alpha$  phase aspect ratio is smaller due to the significant dynamic break-down of  $\alpha$  phase for both the samples compressed along normal direction and rolling direction. With larger deformation, the strip primary  $\alpha$  phase aspect ratio is greater for both the samples compressed along normal direction and rolling direction.

3) The difference on primary  $\alpha$  phase aspect ratio between ND-section and RD-section drops after compression along different directions in two loading passes, suggesting the equiaxity of primary  $\alpha$  phase is improved after deformation. It can be speculated that multi-directional forging can be served as an effective scheme to equiaxify the elongated  $\alpha$  phases of TA15 titanium alloy.

## References

- [1] XU Wen-chen, SHAN De-bin, YANG Guo-ping, LÜ Yan. Flow behavior and microstructure evolution during hot compress of TA15 titanium alloy [J]. Transactions of Nonferrous Metals Society of China, 2006, 16(S3): s2066–s2071.
- [2] ZHU Jing-chuan, WANG Yang, LIU Yong, LAI Zhong-hong, ZHAN Jia-jun. Influence of deformation parameters on microstructure and mechanical properties of TA15 titanium alloy [J]. Transactions of Nonferrous Metals Society of China, 2007, 17: s490–s494.
- [3] CHEN Yong, XU Wen-chen, SHAN De-bin, GUO Bin. Microstructure evolution of TA15 titanium alloy during hot power spinning [J]. Transactions of Nonferrous Metals Society of China, 2011, 21: s323–s327.
- [4] BOYER R R. An overview on the use of titanium in the aerospace industry [J]. Materials Science and Engineering A, 1996, 213: 103–114.
- [5] SHEN G, DAVID F. Manufacturing of aerospace forgings [J]. Journal of Materials Processing Technology, 2000, 98: 189–195.
- [6] WANG Guo, HUI Song-xiao, YE Wen-jun, MI Xu-jun. Hot compressive behavior of Ti–3.0Al–3.7Cr–2.0Fe–0.1B titanium alloy [J]. Transactions of Nonferrous Metals Society of China, 2012, 22: 2965–2971.
- [7] JIANG Shao-song, LU Zhen, HE Xiao-dong, WANG Guo-feng, ZHANG Kai-feng. Superplastic forming Ti–6Al–4V titanium alloy cylinder with near uniform thickness distribution [J]. Transactions of Nonferrous Metals Society of China, 2012, 22: s472–s478.
- [8] SUN Z C, YANG H. Microstructure and mechanical properties of TA15 titanium alloy under multi-step local loading forming [J]. Materials Science and Engineering A, 2009, 523(1–2): 184–192.
- [9] TAMIRISAKANDALA S, VEDAM B V, BHAT R B. Recent advances in the deformation processing of titanium alloys [J]. Journal of Materials Engineering and Performance, 2003, 12: 661–673.

- [10] SEMIATIN S L, SEETHARAMAN V, WEISS I. The thermomechanical processing of alpha/beta titanium alloys [J]. JOM, 1997, 49: 33–39.
- [11] YU Wei-xin, LI Miao-quan, LUO Jiao. Effect of processing parameters on microstructure and mechanical properties in high temperature deformation of Ti–6Al–4V alloy [J]. Rare Metal Materials and Engineering, 2009, 38(1): 19–24. (in Chinese)
- [12] LU Shi-qiang, LI Xin, WANG Ke-lu, DONG Xian-juan, FU M W. High temperature deformation behavior and optimization of hot compression process parameters in TC11 titanium alloy with coarse lamellar original microstructure [J]. Transactions of Nonferrous Metals Society of China, 2013, 23: 353–360.
- [13] SUN Sheng-di, ZONG Ying-ying, SHAN De-bin, GUO Bin. Hot deformation behavior and microstructure evolution of TC4 titanium alloy [J]. Transactions of Nonferrous Metals Society of China, 2010, 20(11): 2181–2184.
- [14] CHEN Hui-qin, CAO Chun-xiao. Characterization of hot deformation microstructures of alpha-beta titanium alloy with equiaxed structure [J]. Transactions of Nonferrous Metals Society of China, 2012, 22(3): 503–509.
- [15] WANG Tao, GUO Hong-zhen, WANG Yan-wei, YAO Ze-kun. Influence of processing parameters on microstructure and tensile properties of TG6 titanium alloy [J]. Materials Science and Engineering A, 2010, 528: 736–744.
- [16] ZONG Y Y, SHAN D B, XU M, LV Y. Flow softening and microstructural evolution of TC11 titanium alloy during hot deformation [J]. Journal of Materials Processing Technology, 2009, 209: 1988–1994.
- [17] JEOUNG H K, SEMIATIN S L, CHONG S L. High-temperature deformation and grain-boundary characteristics of titanium alloys with an equiaxed microstructure [J]. Materials Science and Engineering A, 2008, 45: 601–612.
- [18] FAN X G, GAO P F, YANG H. Microstructure evolution of the transitional region in isothermal local loading of TA15 titanium alloy [J]. Materials Science and Engineering A, 2011, 528(6): 2694–2703.
- [19] GAO P F, YANG H, FAN X G. Quantitative analysis of the microstructure of transitional region under multi-heat isothermal local loading forming of TA15 titanium alloy [J]. Materials and Design, 2011, 32(4): 2012–2020.
- [20] SEMIATIN S L, MONTHEILLET F, SHEN G, JONAS J J. Self-consistent modeling of the flow behavior of wrought alpha/beta titanium alloys under isothermal and nonisothermal hot-working conditions [J]. Metallurgical and Materials Transaction A, 2002, 33: 2719–2727.
- [21] FAN X G, YANG H. Internal-state-variable based self-consistent constitutive modeling for hot working of two-phase titanium alloys coupling microstructure evolution [J]. International Journal of Plasticity, 2011, 27(11): 1833–1852.
- [22] HE D, ZHU J C, LAI Z H, LIU Y, YANG W X. An experimental study of deformation mechanism and microstructure evolution during hot deformation of Ti–6Al–2Zr–1Mo–1V alloy [J]. Materials and Design, 2013, 46(1): 38–48.

## 大型 TA15 钛合金板坯热加工中 $\alpha$ 相形态演变

樊晓光, 杨合, 高鹏飞, 严思梁

西北工业大学 材料学院, 凝固技术国家重点实验室, 西安 710072

**摘要:** 通过不同取向截面上的组织观测及定量金相分析, 研究具有拉长  $\alpha$  相的 TA15 钛合金板坯在两相区热加工中组织形态的演变机制。结果表明: 变形后组织形态主要由加载方向决定; 沿法线方向加载时, 垂直于法线方向截面上的组织为等轴  $\alpha$  相, 而垂直于轧向截面上的组织沿切向拉长的条状  $\alpha$  相; 沿轧向加载时, 垂直于法线方向截面上的组织为沿切向拉长的条状  $\alpha$  相, 而垂直于轧向截面上的组织为条状  $\alpha$  相与宽带状  $\alpha$  相混合的不均匀组织。变形温度较低时, 由于  $\alpha$  相的动态破碎, 条状  $\alpha$  相的轴比较小。变换加载方向进行两道次加载(先法向后轧向或先轧向后法向)时, 两个截面上初生  $\alpha$  相的轴比差较初始组织减小, 等轴度有所提高。

**关键词:** 组织形态; TA15 钛合金; 拉长  $\alpha$  相; 两相区热加工

(Edited by Chao WANG)